Turkish Computational and Theoretical Chemistry

Turkish Comp Theo Chem (TC&TC)

Volume(Issue): 8(4) – Year: 2024 – Pages: 36-47

e-ISSN: 2602-3237

https://doi.org/10.33435/tcandtc.1382029

Received: 30.10.2023 ***Accepted***: 03.03.2024 *Research Article*

Theoretical Study of Khellin Derivatives as Corrosion Inhibitors Based on Density Functional Theory (DFT)

Lidia Gusfi Marni[a], Emriadi Emriadi[b,1], Syukri Darajat[b], Imelda Imelda[b], Khoiriah Khoiriah[c,2]

[a]Department of Chemistry, Islamic University of Sulthan Thaha Saifuddin Jambi, Jambi-36361, Indonesia.
[b]Department of Chemistry, Andalas University, Limau Manis Padang-25163, Indonesia.
[c]Research Centre for Chemistry, National Research and Innovation Agency, Serpong, Indonesia

Abstract: Theoretical studies of Khellin in the presence of electron donor and electron-withdrawing groups as a corrosion inhibitor are investigated using the Density Functional Theory (DFT) with basis set B3LYP/6-31G (d, p) theory level with Gaussian software. This research focuses on the correlation between corrosion inhibition efficiency (EI%) and quantum chemical parameters such as E_{HOMO} (Highest Occupied Molecular Orbital Energy), E_{LUMO} (Lowest Unoccupied Molecular Orbital Energy), energy gap (ΔE), dipole moment (μ), absolute hardness (η), absolute softness (σ), the absolute electronegativity (χ), the fractions of electrons transferred from the inhibitor molecule to the metallic atom (ΔN), the electrophilicity index (ω), total energy (E_T) and theoretical corrosion inhibition efficiency (EI %). The generated results show that the electron-donating groups increase the corrosion inhibition efficiency of Khellin in the sequence $-NH_2 > -SH > -H > -NCH_2 > -NO_2$. The highest corrosion inhibition efficiency obtained about 98.40% proves that NH_2-Khellin is the best corrosion inhibitor of iron. The Moleculer Dinamic (MD) simulation shows good interaction and strong binding energy between Khellin-NH_2 and Fe (110) surface.

Keywords: Quantum chemical calculation, DFT, Khellin, Substituent effect, Corrosion Inhibitors

1. Introduction

The process of reducing a material's quality and useful life—mostly metal—through electrochemical reactions in a hostile environment is known as corrosion. The National Association of Corrosion Engineers (NACE) reports that annual corrosion expenditures surpass 2.5 trillion dollars worldwide [1]. Other issues including safety, environmental harm, and security are also brought on by corrosion in addition to economic ones [2]. Using an anti-corrosion agent inhibitor to decrease the corrosion rate is the solution to this issue. Approximately 35% of expenses can be saved annually by using inhibitor technology [3].

Organic natural inhibitors are currently widely developed because they are inexpensive, effective, biodegradable, renewable, and have a high anti-corrosion efficiency [4]. Compounds with heteroatomic groups (O, N, S, and P), aromatic rings [5], electronegative structures [6], as well as secondary metabolite compounds like alkaloids, flavonoids, lignin, and tannins, are the most effective and efficient as natural corrosion inhibitors. Inhibitor molecules with appropriate functional groups can be adsorbed chemically or physically by the complexes and electrostatic bond formation [6]. The inhibitor molecule's structure, steric factors, aromatics, electron density on the donor atom, and the existence of functional groups (C = NH, -N =N-, -CHO, R -OH, C = C) have an impact on the inhibitor's adsorption [7]. Theoretical and experimental Lidya studies have reported that

---

[1] Corresponding Authors

e-mail: emriadi@sci.unand.ac.id

[2] Corresponding Authors

e-mail: khoi013@brin.go.id

the Khellin compound found in Ammi visnaga is effective as an iron inhibitor [8, 9]. The oxygen atom's lone pair of electrons allows khelin to be adsorbed on metal surfaces.

One of the best computational calculation techniques, density functional theory (DFT), is frequently applied in studies design of corrosion and cancer inhibitors [10-12]. This simple technique can predict the corrosion inhibitory reactivity and identify molecular active sites. For comprehending molecular characteristics and explaining how atoms behave in molecules, DFT is a helpful tool [1,13-17]. It offers particular details about charge and energy transfer phenomena, atomic-scale electronic characteristics, molecular structure, and interaction mechanisms of molecules adhering to surfaces [1,18-20]. Additionally, to comprehend the nature of the surface-corrosion inhibitor reaction at the electron surface [17,21].

The purpose of this study is to investigate the iron corrosion-inhibiting properties of compounds derived from Khellin. This study uses the DFT method as a theoretical approach due to its accuracy, shorter computational time [22]. It is anticipated that this theoretical approach will support experimental research and offer more thorough insight into the precise, efficient, and effective design of corrosion inhibitors on compounds derived from Khellin.

2. Computational Method

2.1. DFT Calculations

All theoretical calculations were performed using the density functional theory (DFT), a common method used in predicting the chemical reactivity of molecules. In this research, the input files of studied molecules were prepared with Gauss View 5.0.8 [23]. DFT calculations were carried out using Gaussian 16 software with three hybrid exchange functional parameters and Beck, Lee-Yang-Parr (B3LYP) basis set 6-31G (d, p) [24]. The molecules studied have been studied both in the presence of electron donor and electron-withdrawing groups. The calculation of quantum chemical parameters is Highest Occupied Molecular Orbital Energy (E_{HOMO}), Lowest Unoccupied Molecular Orbital Energy (E_{LUMO}), energy gap (ΔE), dipole moment (μ), absolute hardness (η), absolute softness (σ), the absolute electronegativity (χ), the fractions of electrons transferred from the inhibitor molecule to the metallic atom (ΔN), the electrophilicity index (ω), total energy (ET) and theoretical corrosion inhibition efficiency (EI%) as reported [22, 25-27].

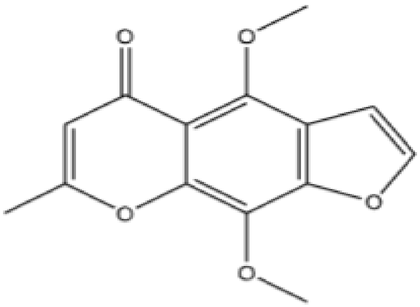

Figure 1. The structure and schematic representation of Khellin derivatives, (R1 = $-NH_2$, -SH, $-NCH_2$, $-NO_2$), and R2 = -H

According to Koopman's theorem, the E_{HOMO} and the E_{LUMO} are used to demonstrate I, A, η, and **χ** [28]. Ionization potential (I) is the number of energy needed to remove one electron from a molecule. Electron affinity (A) is defined as the amount of releasing energy when a proton is introduced into a system. Both I and A are associated with the E_{HOMO} and the E_{LUMO} through Eqn. 1 and Eqn. 2 [13]. In numerical applications, I and A are important to calculate the chemical potential of dipole moment (μ) and global hardness (η). Then, gap energy (ΔE) is a function of the inhibitor molecules' reactivity adsorbed on the metal surface and calculated by using Eqn. 3 [13].

$$I = -E_{HOMO} \qquad \textbf{Eqn. 1}$$

$$A = -E_{LUMO} \qquad \textbf{Eqn. 2}$$

$$\Delta E = E_{HOMO} - E_{LUMO} \qquad \textbf{Eqn. 3}$$

Electronegativity (χ) is the ability of an atom or group of atoms to attract electrons toward it [29]. The electronegativity formula (χ) is described by Eqn. 4 below:

$$\chi = \frac{I + A}{2} = -\frac{1}{2}(E_{HOMO} + E_{LUMO}) \qquad \textbf{Eqn. 4}$$

Global hardness (η) is an indicator of an atom 'resistance to a charge transfer. Whereas, global softness (σ) is the inverse of global hardness, electron polarizability, an ability of atoms or groups of atoms to accept electrons. Two of these parameters are calculated using Eqn. 5 and Eqn. 6.

$$\eta = \frac{I - A}{2} = -\frac{1}{2}(E_{HOMO} - E_{LUMO}) \qquad \text{Eqn. 5}$$

$$\sigma = \frac{1}{\eta} = -\left(\frac{2}{E_{HOMO} - E_{LUMO}}\right) \qquad \text{Eqn. 6}$$

According to Parr, electrophilicity (ω) is a reactivity descriptor quantitatively related to the electrophilic nature of a molecule on a relative scale. Electrophilicity (ω) is a minimum energy reference with the maximum electron flow between the donor and the electron acceptor [24]. It is determined by using Eqn. 7:

$$\omega = \frac{\mu^2}{2\eta} \qquad \text{Eqn. 7}$$

The electronic flow will occur from the molecule with the lower electronegativity toward that of higher value, until the chemical potential is the same. The fraction of transferred electron from Khellin derivates to iron atom is counted by Eqn. 8. [30]:

$$\Delta N = \frac{\chi_{Fe} - \chi_{inh}}{2(\eta_{Fe} + \eta_{inh})} \qquad \textbf{Eqn. 8}$$

Where χ_{Fe} and χ_{inh} represent the absolute electronegativity of each iron molecule (Fe) and inhibitor. Then, the terms of η_{Fe} and η_{inh} signified iron and inhibitor molecule's absolute hardness. The transported electron fraction is calculated using theoretical data, for bulk iron electronegativity (Fe = 7.0 eV) and global hardness ($\eta_{Fe} = 0$) by assuming that for metal mass I = A [27, 31]. The value of corrosion inhibition efficiency (IE %) is also calculated using Eqn. 9-11 below:

$$\mathbf{I_{add\%}} = \frac{\mathbf{I_{inhibitor} - 1(x - inhibitor)}}{\mathbf{I_{inhibitor}}} \boldsymbol{\chi}\, \mathbf{100\%} \qquad \text{Eqn. 9}$$

$$\mathbf{I_{eadd\%}} = \mathbf{I_{add\%}} \times \times \mathbf{I_{exp\%}} \qquad \text{Eqn. 10}$$

$$\mathbf{IE_{theory\%}} = \mathbf{IE_{exp\%}} \times \times \mathbf{I_{eadd\%}} \qquad \text{Eqn. 11}$$

Where, I_{add}%, I_{eadd}%, IE_{exp}%, and IE $_{theory\%}$ are the ionization potential percentage of an inhibitor compound, the corrosion inhibition efficiency of inhibitor compounds (Khellin derivatives), the corrosion inhibition efficiency of experimental results, and the theoretical efficiency of corrosion inhibition inhibitors [32], respectively.

1.2 Molecular Dynamics Simulation

MD simulations were conducted on all compounds to explore their interactions with an iron surface using the Forcite module in BIOVIA Materials Studio 2017. The simulations took place within a box measuring (28.66 Å × 28.66 Å × 45.76 Å) with periodic boundary conditions, comprising six layers of cleaved iron Fe (110) forming a 10 × 10 supercell. The Fe (110) plane is deemed the most stable iron surface due to its dense arrangement [33]. A 30 Å vacuum layer was positioned directly above the iron surface and filled with each inhibitor compound alongside 100 H_2O molecules to simulated a real corrosive environment. The COMPASS force field was utilized for geometry optimization of all component structures within the box. Energy interaction of the compound inhibitor corrosion with the metal surface using Eqn 12.

$$E_{interaksi} = E_{kompleks} - E_{Fe} - E_{inhibitor} \qquad \textbf{Eqn. 12}$$

E_{total} is the single point energy of all components in the simulation box, $E_{Fe+solution}$ is the energy of iron (110) surface and the H_2O and $E_{inhibitor}$ is the single point energy of the inhibitor. The binding energy ($E_{binding}$) was obtained with Eqn 13.

$$E_{binding} = -E_{interaction} \qquad \textbf{Eqn. 13}$$

3. Results and discussion

3.1. Quantum Chemical Calculations

Calculations were performed to determine the active sites and local reactivity of all molecules studied. Geometric optimisations using the B3LYP function and basis set 6-31G (d, p) were carried out. For the Khellin derivative molecule, two types of substituents were chosen: electron-donating (NH_2, SH, H) and electron-withdrawing (NCH_2, $-NO_2$). They were inserted into the Khellin structure, as shown in Fig. 1. Their presence will affect the corrosion inhibition efficiency of organic compounds by replacing the H atom attached to the ring C.

As previously stated, quantum chemical parameters are primarily calculated to assess the ability of their inhibition properties. When there are molecular donor and acceptor processes in the HOMO and LUMO orbitals, electron transition occurs. E_{HOMO} refers to molecules' proclivity to donate electrons [28]. Table 1 shows that electron-donating have higher E_{HOMO} than electron withdrawing groups. The highest value obtained by NH_2 as a substituent is approximately -0.1945 eV, and the lowest value obtained by NO_2 is approximately -0.2140 eV. This value indicates that the electron-donating substituent will donate more electrons than the electron-drawing group. The higher the E_{HOMO} value, the more capable organic molecules are of attaching metal cations and the greater the corrosion inhibition efficiency [26, 34]. A decrease in the Egap value and an easier for the molecule to bind to the metal surface are indicated by an increase in the E_{HOMO} value [21, 35, 36]. Hadisaputra [34] reports a similar trend in his research on benzylnicotine derivatives as corrosion inhibitors.

When determining the reactivity of inhibitor molecules for adsorption on the iron surface, the energy gap (ΔE) is a crucial parameter. As indicated in Table 1, Khellin-NH_2 has ΔE = 0.1453 eV, which is lower than Khellin-NH_2 ΔE = 0.1455 eV and other derivatives. The low energy required to remove electrons from the last occupied orbital means that a low ΔE value will result in good inhibition efficiency [25]. Furthermore, low-ΔE molecules exhibit greater polarisation, high chemical activity, and low kinetic stability; these molecules are referred to as soft molecules [37]. These findings demonstrate the effectiveness of Khellin-NH_2 as a corrosion inhibitor.

Another principal electronic parameter for assessing an atom or molecule's degree of chemical reactivity is its ionisation potential (I). Compared to electron-withdrawing groups, electron donor groups have a lower I value. In comparison to the NO_2 substituent (0.2140 eV), the NH_2 substituent yields a lower I value (0.1945 eV), suggesting that the NH_2 substituent enhances Khellin reactivity to the metal surfaces. Small ionisation potential values make the electrons easier to separate from molecules, while high ones make it difficult to form bonds with metals due to stability and inert [30, 38].

The electronegativity value (χ) is also shown in Table 1. With the sequence NH_2> SH > H > NCH_2 > NO_2, the electron donor groups substituent gives a higher value than the electron withdrawing groups. According to the value, Khellin-NH_2 (-0.1412 eV) is more electronegative than NO_2 is -0.1219 eV. A high electronegativity value makes the Khellin-NH_2 molecules easily to attract electrons and be adsorbed on metal surfaces [14].

The global hardness is the next important parameter. Table 1 shows the order of global hardness values from highest to lowest: NO_2 > NCH_2 > H > SH > NH_2. The global hardness is inversely proportional to the global softness. According to the data obtained, the NH_2 molecule causes Khellin to be globally soft, easily react, and form coordination bonds with the metal surface, increasing the efficiency of corrosion inhibition. This data supports Pearson's [30] finding that a molecule with a higher global softness value has difficulty reacting with metal surfaces, whereas a molecule with a higher global softness value does not. TÜZÜN also believes that high global hardness values make the electron donor process difficult [15, 38]. These two characteristics are correlated to the energy gap value (ΔE). The soft molecules with a small energy gap produce electrons more easily and they can be used as corrosion inhibitors [15].

The electrons transferred number (ΔN) values calculated are as follows: NH_2 > H > NCH_2 > SH > NO_2. The highest corrosion inhibition efficiency is predicted to be obtained by NH_2 (0.2987). The contrast result obtained was NO_2 substituent (0.2578). If the ΔN is <3.6, the corrosion inhibition efficiency increases by increasing the molecule's ability to donate electrons to the metal surface [25]. The positive sign of the value then explains how electron transfer from the molecule to the iron surface occurs [21].

Table 1. The quantum chemical parameters result of Khellin derivates by DFT B3LYP/6-31G base set

Parameters	**NH_2**	**SH**	**H**	**NCH_2**	**NO_2**
E_{HOMO} (eV)	-0.1945	-0.1966	-0.2049	-0.2105	-0.2140
E_{LUMO} (eV)	-0.0492	-0.0480	-0.0411	-0.0539	-0.0685
Energi Gap/ΔE (eV)	0.1453	0.1485	0.1638	0.1565	0.1455
Dipol moment/μ (Debye)	2.3309	4.4350	3.6455	3.2863	8.2024
Ionization potential/I (eV)	0.1945	0.1966	0.2049	0.2105	0.2138
Electron Affinity/A (eV)	0.0492	0,0480	0.0411	0.0539	0.0685
Electronegativity/χ (eV)	-0.1219	-0.1223	-0.1229	-0.1322	-0.1412
Global Hardness η (eV)	0.0726	0.0743	0.0818	0.0783	0.0727
Global Softness/σ (eV^{-1})	13.7637	13.4625	12.2144	12.7738	13.7447
Electrophilicity/ω (D^2/eV)	37.3896	132.3992	81.1632	68.9772	462.3693

Electron transfer/ΔN	0.2987	0.2645	0.2916	0.2791	0.2598
Total energy (a.u)	-972.1542	-1314.9827	-877.4916	-1010.2325	-1121.2769

Table 2. The corrosion inhibition efficiency (IE %) of Khellin derivatives

Substituents	**Ionization potential (eV)**	**Electron affinity (eV)**	**I_{add} %**	**I_{eadd} %**	**Increase efficiency %**	**Inhibition efficiency**	
						Theory %	**Experiments %**
Khellin	0.2000	0.0381	-0.0245	-2.3471	-	95.8	95.8[a]
NH_2	0.1945	0.0492	0.02715	2.60097	2.64	98.40	-
SH	0.1966	0.0480	0.0168	1.60944	1.65	97.41	-
H	0.2049	0.0411	-0.079	-7.5682	1.65	93.4	-
NCH_2	0.2105	0.0539	-0.0528	-5.05824	-5.57	90.74	-
NO_2	0.2138	0.0685	-0.069	-6.6102	-7.41	89.19	-

[a][39]

Table.1 also conveys electrophilicity (ω). This parameter, along with the opposite term nucleophilicity (ε)/(1/ω), is used to determine the tendency of inhibitor molecules to accept electrons. This parameter's calculation yields Khellin-NH_2 as the lowest electrophilicity of 37.3896 D^2/eV which indicates a nucleophile and more effective as a corrosion inhibitor than other derivates. Molecules with a high nucleophilicity value are effective corrosion inhibitors [15].

Table 2 shows the theoretical calculation result of corrosion inhibition efficiency using DFT with equations (9)-(11). The electron donor groups have higher efficiency (93.4%-98.40%) than the electron-withdrawing groups (89.19%-90.74%). The efficiency of Khellin is reduced about -7.41% with NO_2 as a substituent. However, the presence of NH_2 increases the efficiency about 2.64%. Based on the results of quantum chemical parameters and inhibition efficiency, the NH_2 substituent molecule is the best potential corrosion inhibitor. This result is consistent with previous findings that the addition of nitration groups (NO_2) reduces inhibition efficiency [32].

Table 3. Visualization of HOMO-LUMO energies and electrostatic potential of Khellin derivatives

	HOMO	**LUMO**	**ESP**
-NH_2	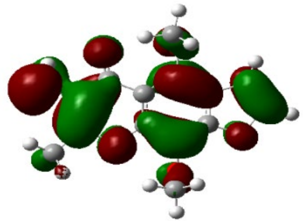	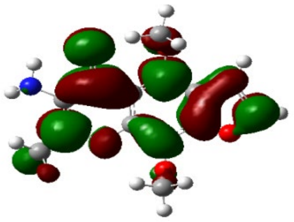	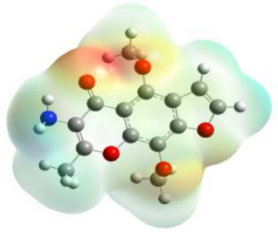
-SH	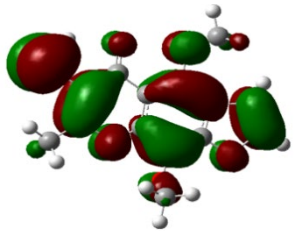	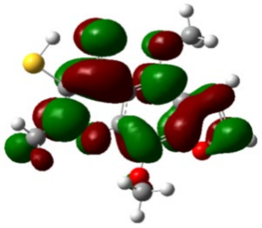	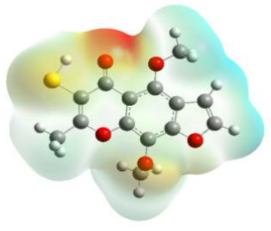
-NCH_2	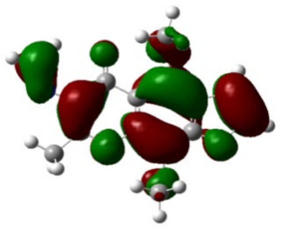	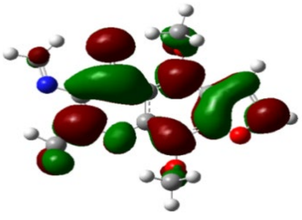	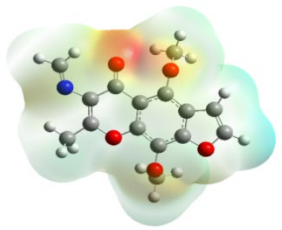

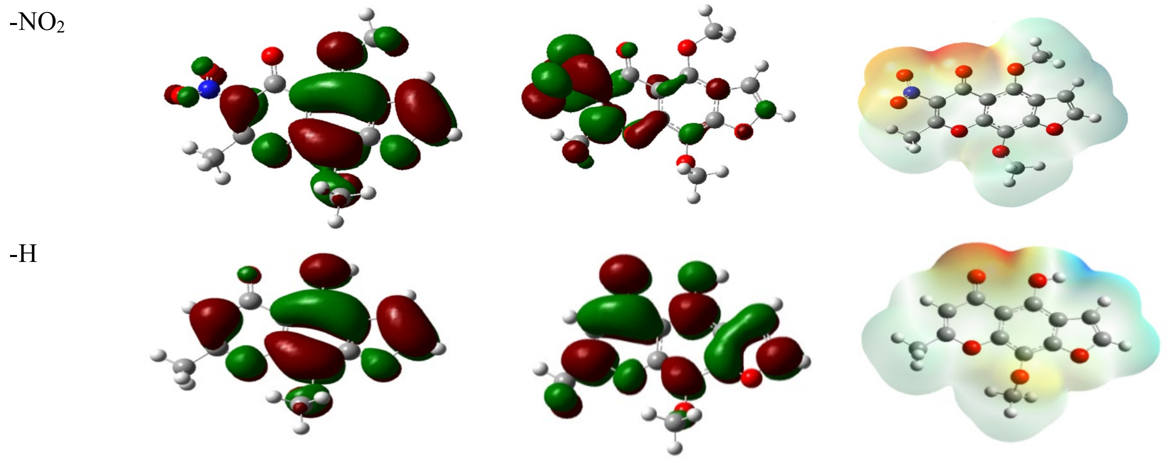

Table 4. Mulliken charge of Khellin derivatives

Khellin-NH_2		Khellin-SH		Khellin-H		Khellin-NCH_2		Khellin-NO_2	
1 C	0.165440	1 C	-0.211287	1 C	-0.185042	1 C	0.170484	1 C	0.111466
2 C	0.412754	2 C	0.433519	2 C	0.418098	2 C	0.430753	2 C	0.442129
3 C	0.049227	3 C	0.028820	3 C	0.029799	3 C	0.041865	3 C	0.015326
4 C	0.224715	4 C	0.235733	4 C	0.232471	4 C	0.218553	4 C	0.218207
5 C	0.291803	5 C	0.315841	5 C	0.336847	5 C	0.300157	5 C	0.368788
6 C	0.218792	6 C	0.238223	6 H	0.102791	6 C	0.219928	6 C	0.237645
7 C	0.250600	7 C	0.236190	7 C	0.210338	7 C	0.256580	5 C	0.251743
8 C	0.287691	8 C	0.289391	8 C	0.241444	8 C	0.287414	8 C	0.291176
9 C	0.098326	9 C	0.080628	9 C	0.290903	9 C	0.100437	9 C	0.099987
10 C	-0.143210	10 C	-0.146814	10 C	0.077497	10 C	-0.143279	10 C	-0.211715
11 C	0.127735	11 C	0.126668	11 C	-0.164774	11 C	0.128639	11 C	0.082575
12 O	-0.488799	12 O	-0.481726	12 C	0.132977	12 O	-0.486871	12 O	-0.479047
13 O	-0.530096	13 O	-0.483395	13 O	-0.483758	13 O	-0.528197	13 O	-0.467383
14 O	-0.529819	14 O	-0.519640	14 O	-0.520141	14 O	-0.517762	14 O	-0.511948
15 O	-0.548881	15 O	-0.511006	15 O	-0.527470	15 O	-0.531379	15 O	-0.471820
16 C	-0.079982	16 C	-0.082225	16 O	-0.500755	16 C	-0.078530	16 C	-0.223015
17 H	0.139287	17 H	0.116017	17 H	0.123331	17 H	0.137376	17 H	0.157803
18 H	0.093044	18 H	0.117452	18 H	0.102549	18 H	0.093317	18 H	0.159216
19 H	0.116749	19 H	0.137229	19 C	-0.374438	19 H	0.118536	19 H	0.189264
20 H	0.120130	20 H	0.122330	20 H	0.143250	20 H	0.122472	20 H	0.171367
21 H	0.114888	21 H	0.103742	21 H	0.136641	21 H	0.116887	21 H	0.154582
22 C	-0.386631	22 C	-0.384438	22 H	0.130959	22 C	-0.366392	22 C	-0.512747
23 H	0.135840	23 H	0.147945	23 O	**-0.537594**	23 H	0.139716	23 H	0.199784
24 H	0.133376	24 H	0.133899	24 C	-0.076720	24 H	0.128518	24 H	0.184707
25 H	0.139702	25 H	0.147305	25 H	0.108370	25 H	0.163558	25 H	0.195919
26 O	-0.537375	26 O	**-0.536588**	26 H	0.111529	26 O	**-0.537123**	26 O	**-0.526187**
27 C	-0.078519	27 C	-0.077357	27 H	0.122099	27 C	-0.079584	27 C	-0.219210
28 H	0.109236	28 H	0.109887	28 H	0.318798	28 H	0.110752	28 H	0.163696
29 H	0.113558	29 H	0.111366			29 H	0.113697	29 H	0.149973
30 H	0.122853	30 H	0.123189			30 H	0.125643	30 H	0.169774

31 N	**- 0.673667**	**31 S**	-0.038042			**31 N**	-0.454805	**31 N**	0.356764
32 H	0.253823	**32 H**	0.117144			**32 C**	-0.037364	**32 O**	-0.398119
33 H	0.277411					**33 H**	0.143918	**33 O**	-0.350698
						34 H	0.092091		

The distribution of molecular orbital densities calculated using set B3LYP/6-31G(d,p) to determine a molecule's relative polarity is shown in Table 3. In terms of size, shape, charge density, and chemical reactivity site, the electron surface density of five Khellin derivative molecules is mapped to the electrostatic potential surface [15]. The electron donor substituent's inductive effect distributes electron density in the aromatic system and brings it closer to the oxygen carbonyl atom. The presence of electron donor groups in the HOMO region of the khellin indicates that electrons are primarily localised in the substituent region, specifically in the N-H_2, S-H, H bonds, oxygen atoms, and C=C bonds in the pyran ring.

Meanwhile, the presence of electron-withdrawing substituents causes electrons to be localized in the C-O bond of the pyran ring and the C=C bond in the furan ring as shown in Table 3. These atoms are predicted to be the interaction center between inhibitor molecules and the metal surface. The atoms in the HOMO region act as electron donors from the inhibitor molecule to form a coordination bond with the metal surface. Then, at the LUMO region in Table 3, the presence of electron donor groups leads electrons to be localized in the C-O bond in the furan ring, the C=C bond in the benzene ring, the carbon atom in the pyran ring, the C-C bond, and the C=C bond.

Meantime, the electrons are distributed to the O atom, C-C bond in the pyran ring, C-C bond in the furan ring at the LUMO region for the Khellin-NCH_2 molecule, and distributed to NO_2 bond for the Khellin-NO_2 molecule. According to Gece and Bilgiç, these atoms are responsible for accepting electrons from metal orbitals [25] that the strength of molecular adsorption on HOMO and LUMO orbitals is comparable. Table 3 depicts the electron distribution in the electrostatic potential region (ESP). The different colours represented the electrostatic potential region. The potential increases in the order of red <orange <yellow <green <blue. The more negative an atom's charge, the more reactive is with the metal surface by donating an electron [40].

Table 4 clearly shows that nitrogen and carbon atoms with negative charges could offer electrons to form bonds with the metal surface. The molecule khellin-NH_2 contains more electronegative atoms than other substituents. It has the lowest N_31 (-0.673667), indicating that the atom donates more electrons and has a higher inhibitory efficiency.

The data also suggests that the area with the highest electron density is the centre of the attacking electrophile [16]. Atomic N, O, and C are active centres strongly bonded to metal surfaces. Furthermore, the N atom of Khellin-NH_2 is more negative than that of Khellin-NCH_2 and Khellin-NO_2. Even the N atom in Khellin-NO_2 has a positive charge. It is clear from Table 4 that Nitrogen and Carbon atoms carrying negative charges could offer electrons to form bonds with the metal surface. Molecule khellin-NH_2 has some more electronegative atoms compared to other substituents. It has the lowest N_31 (-0.673667) as an indication that the atom donates more electrons and has a higher inhibitory efficiency than the other substituents.

The data also suggests the area with the highest electron density is the center of the attacking electrophile [16]. Atomic N, O, and C are active centers that are strongly bonded to metal surfaces. Further, the N atom of the Khellin-NH_2 is more negative than Khellin NCH_2, and Khellin-NO_2. Even, the N atom of Khellin-NO_2 has positive charges. As a result, Khellin-NH_2 has a highest potential for corrosion inhibition. The more negative the atomic charges of the inhibitors, the more easily the atom donates electrons to the metal's unoccupied orbital and preferentially adsorbs on the metal surface [37]. Furthermore, some positively charged C atoms serve as nucleophile centres. The Khellin derivative molecule can accept a lone pair of electrons from the ion metal via these atoms, giving it a high potential as a corrosion inhibitor on metal surfaces.

3.2. Molecular dynamics (MD) simulation

Dynamic molecular simulation is the best method to explain the adsorption behavior of inhibitors on metal surfaces [41]. Through MD simulations, it is possible to gain deeper insight into how green inhibitors adsorb on metal surfaces and what changes in inhibitors will result in significant differences in corrosion inhibition. Molecular dynamics simulations were carried out on each khellin derivative compound to determine the stable configuration of various inhibitor molecules and their interaction patterns with the Fe (110) surface. This simulation aims to imitate the real world iron corrosion process and also explore processes related to the corrosion inhibitory behavior of molecules in metals [33]. The interaction energy ($E_{interaction}$) and binding energy ($E_{binding}$) of the khellin inhibitor and its derivatives on the Fe (110) surface are shown in Table 4. Meanwhile, Fig. 2 shows the side and top views of the low energy adsorption configuration of the khellin derivative molecule on the Fe (110) surface.

Fig. 2 show all the khellin derivative inhibitor molecules are adsorbed on the iron surface in a horizontal/flat orientation. Central site of inhibitor adsorption on the Fe (110) surface via heteroatom groups, oxygen, Nitrogen and π structure on the aromatic ring; that interact parallel or flat to the iron surface can maximize surface contact. This result ensures the creation of a large surface area to inhibit dissolution of the metal surface. Inhibitor molecules that interact with iron in the flat configuration, act as superior inhibitors.

The adsorption performance of the inhibitor on the iron surface is analysed on the basis of its interaction energy (Einteraction) (see Table 4). A negative value of Einteraction indicates the spontaneous adsorption of inhibitor molecules on the Fe (110) surface. The more negative the interaction energy is, the more positive the binding energy is, making it easier for the molecules to be adsorbed on the iron surface [33].

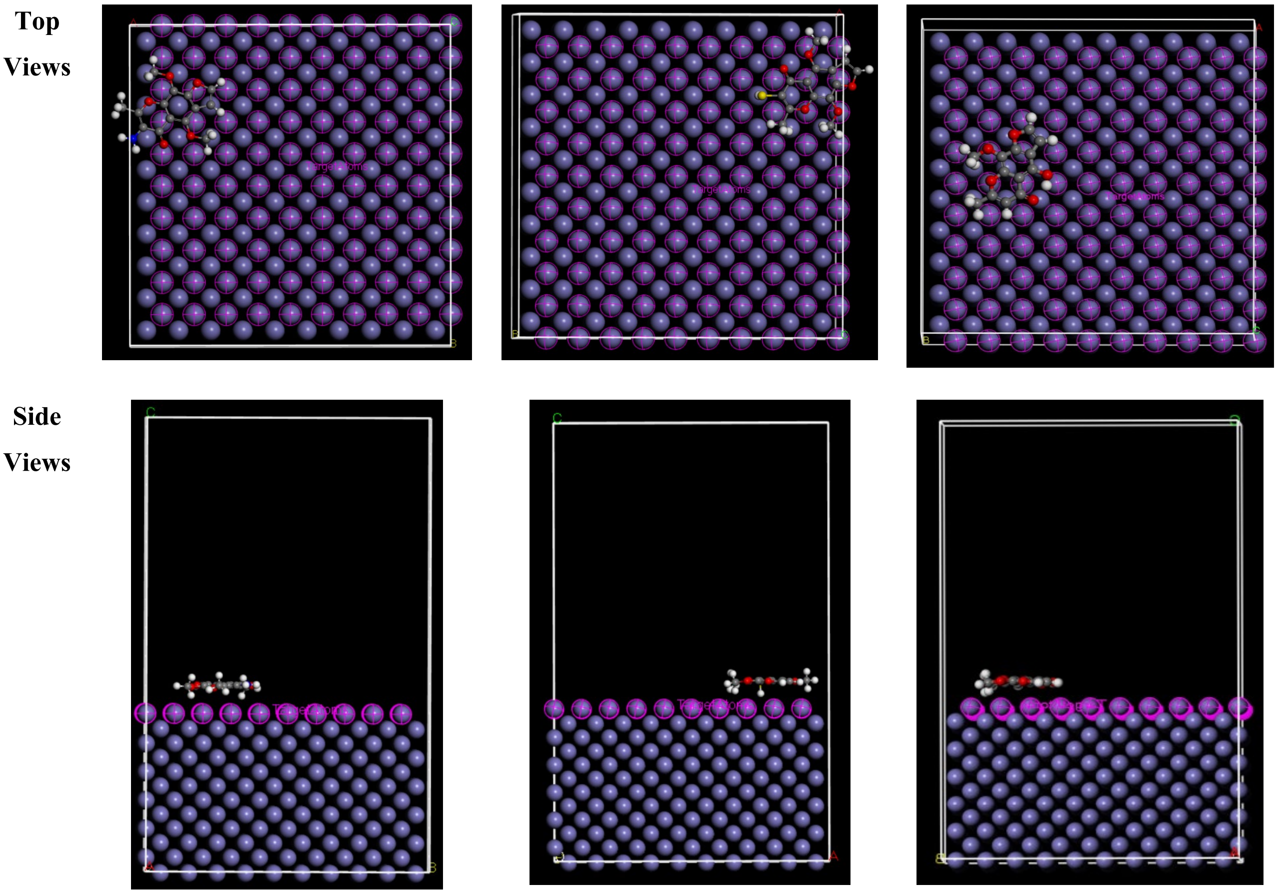

Khellin-NH_2 Khellin-SH Khellin-H

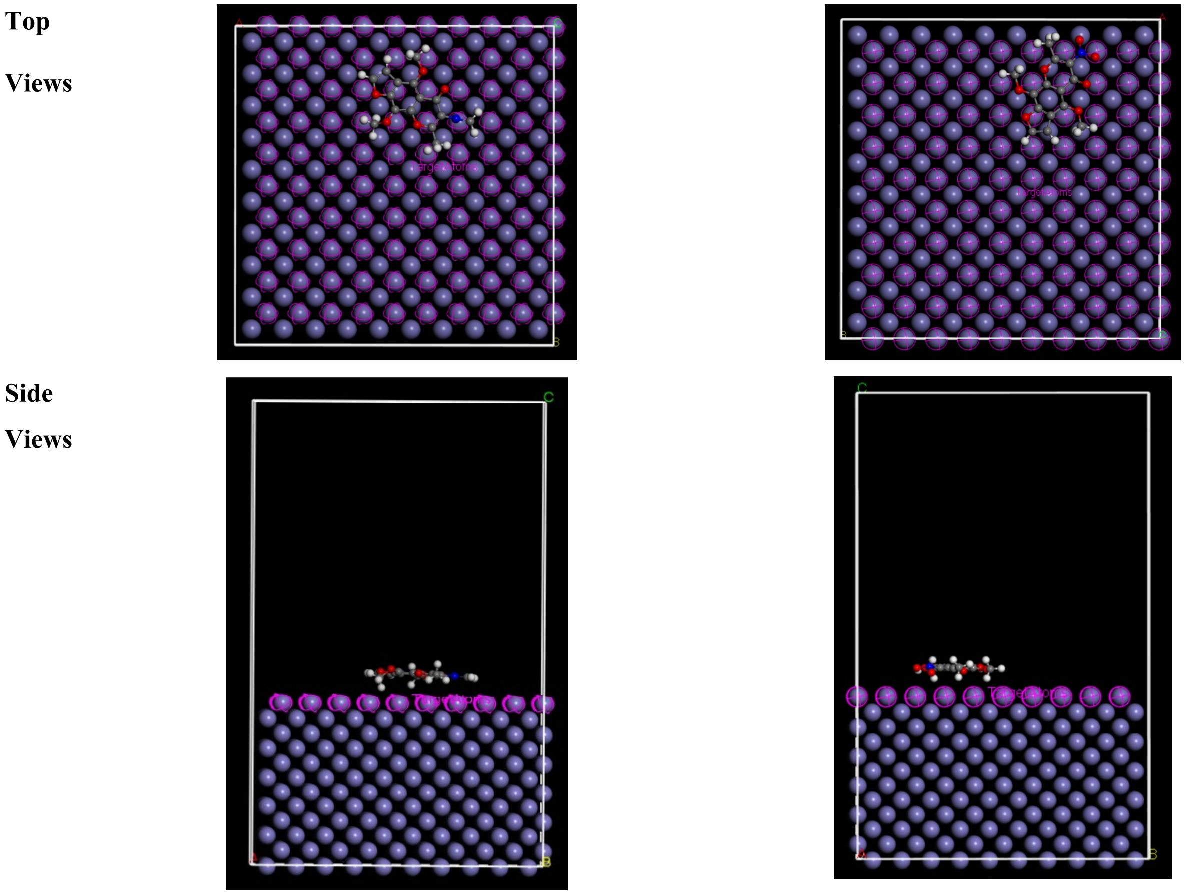

Khellin-NCH_2 Khellin-NO_2

Figure 2. (a) Views side and (b) top presenting the most stable configurations observed in MD simulations for the adsorption of Khellin derivative compounds on the Fe (110) surface.

Table 5. Interaction (adsorption) and binding energies obtained from MD simulation of the Khellin derivatives compounds adsorbed on Fe

Simulation Models	$E_{Interaction}$ (kJ/mol)	$E_{Binding}$ (kJ/mol)
Fe (1 1 0) / Khellin-NH_2	-127,153	127,153
Fe (1 1 0) / Khellin-SH	-100,318	100,318
Fe (1 1 0) / Khellin-H	-85,414	85,414
Fe (1 1 0) / Khellin-NCH_2	-95,124	95,124
Fe (1 1 0) / Khellin-NO_2	-75,234	75,234

According to the results of the MD simulation, the order of interaction energy is as follows: Khellin-NH2 (-127,153 kJ/mol) < Khellin-SH (-100,318 kcal/mol) < Khellin-H (-85,414 kJ/mol) < Khellin-NCH_2 (-95.124 kJ/mol) < Khellin-NO_2 (-75.234 kJ/mol). Khellin-NH_2 has the highest binding energy compared to the other selected molecules, indicating that this compound is most readily adsorbed on iron surfaces and provides the best protection on the surface. This is consistent with the results of the DFT calculations and the percentage inhibition effect obtained. The adsorption of inhibitor molecules on the Fe (110) surface occurs by electron exchange between heteroatom groups and p-systems in the inhibitor and the active surface sites of the Fe (110) metal. This enables the formation of bonds (π-ππ) due to the overlap of free doubles of oxygen, nitrogen and carbon-carbon pi-orbitals on the inhibitor and electrons (3d) of the iron atom [42].

4. Conclusions

This research was carried out as a theoretical study of the anti-corrosion properties of Khellin derivatives on the iron surface by calculating the quantum chemical parameters using DFT calculations. The effect of electron-donating (NH_2, SH, H) and electrons-withdrawing (NCH_2, -NO_2) as Khellin substituents on the efficiency inhibition were investigated. DFT results show molecular orbitals $E_{HOMO)}$ and transferred electron fraction (ΔN) are related to the corrosion inhibition efficiency (IE %). The calculation data informs that electron donor groups (NH_2, SH, H) as Kellin substituens increase the inhibition efficiency. The highest inhibition efficiecy obtained by the NH_2 presence with the order NH_2 > SH > H > NCH_2 > NO_2 on a B3LYP / 6-31G (d, p) base set. This result also supported by MD simulation, where the inhibitor molecules are adsorbed with a flat configuration on Fe metal (1 1 0) and the strong binding energy value obtained from the electron-donating substituent with the iron surface shows good potential anti-corrosion. The findings of this study can be used as a reference for designing Kellin compounds as corrosion inhibitors.

References

[1] D.K. Verma, Density Functional Theory (DFT) as a Powerful Tool for Designing Corrosion Inhibitors in Aqueous Phase, (2018).

[2] A. Sedik, D. Lerari, A. Salci, S. Athmani, K. Bachari, I.H. Gecibesler, R. Solmaz, Dardagan Fruit extract as eco-friendly corrosion inhibitor for mild steel in 1 M HCl: Electrochemical and surface morphological studies, Journal of the Taiwan Institute of Chemical Engineers 107 (2020) 189–200.

[3] Stefania Marzorati, L. Verotta, S.P. Trasatti, Review Green Corrosion Inhibitors from Natural Sources and BiomassWastes, Molecules 24 (48) (2019) 1-24.

[4] L.T. Popoola, Organic green corrosion inhibitors (OGCIs): a critical review, Corrosion Reviews, 37 (2) (2019) 1-34.

[5] Y. Stiadi, S. Arief, H. Aziz, Mai Efdi, Emriadi, Inhibisi korosi baja ringan menggunakan bahan alami dalam medium asam klorida: Review, Jurnal Riset Kimia, 10 (1) (2019) 51-65.

[6] H. Ju, Z.-P. Kai, Y. Li, Aminic nitrogen-bearing polydentate Schiff base compounds as corrosion inhibitors for iron in acidic media: A quantum chemical calculation, Corrosion Science, 50 (3) (2008) 865-871.

[7] I. Zaafarany, M. Abdallah, Ethoxylated Fatty Amide as Corrosion Inhibitors for Carbon Steel in Hydrochloric Acid Solution, International Journal of Electrochemical Science, 5 (1) (2010) 18-28.

[8] L.G. Marni, E. Emriadi, S. Syukri, I. Imelda, Mempelajari inhibisi korosi senyawa khellin dan visnagin pada atom besi menggunakan metode DFT (density functional theory), Jurnal Litbang Industri, 9 (2) (2019) 111.

[9] A.Y. El-Etre, Khillah extract as inhibitor for acid corrosion of SX 316 steel, Applied Surface Science, 252 (24) (2006) 8521-8525.

[10] A. Kumer, U. Chakma, A. Chandro, D. Howlader, S. Akash, M.E. Kobir, T. Hossain, M.M. Matin, Modified d-glucofuranose computationally screening for inhibitor of breast cancer and triple breast cancer: Chemical descriptor, molecular docking, molecular dynamics and QSAR, J. Chil. Chem. Soc., 67 (3) (2022) 5623-5636.

[11] S. Akash, F.I. Aovi, M.A.K. Azad, A. Kumer, U. Chakma, M.R. Islam, N. Mukerjee, M.M. Rahman, I. Bayil, S. Rashid, R. Sharma, A drug design strategy based on molecular docking and molecular dynamics simulations applied to development of inhibitor against triple-negative breast cancer by Scutellarein derivatives, PloS one, 18 (10) (2023) e0283271.

[12] M.E. Kobir, A. Ahmed, M.A.H. Roni, U. Chakma, M.R. Amin, A. Chandro, A. Kumer, Anti-lung cancer drug discovery approaches by polysaccharides: an in silico study, quantum calculation and molecular dynamics study, Journal of biomolecular structure & dynamics, 41 (14) (2023) 6616-6632.

[13] N.O. Obi-Egbedi, N.D. Ojo, Computational studies of the corrosion inhibition potentials of some derivatives of 1H-Imidazo [4, 5-F] [1, 10] phenanthroline, Journal of Science Research 14 (1) (2015) 50-56.

[14] V.M. Udowo, Computational Studies of the Corrosion Inhibition Potentials of Quercetin and Coumarin, Archives of Organic and Inorganic Chemical Sciences, 2 (2) (2018).

[15] B. TÜZÜN, Theoretical Evaluation of Six Indazole Derivatives as Corrosion Inhibitors

Based on DFT, Turkish Computational and Theoretical Chemistry, 2 (1) (2018) 12-22.

[16] V. Kavitha, N. Gunavathy, Theoretical Studies on Corrosion Inhibition Effect o f Coumarin and its Derivatives against Metals u sing Computational Methods, International Journal of Engineering and Techniques 2 (6) (2016) 105-112.

[17] M. Alam, M.N. Abser, A. Kumer, M.M.H. Bhuiyan, P. Akter, M.E. Hossain, U. Chakma, Synthesis, characterization, antibacterial activity of thiosemicarbazones derivatives and their computational approaches: Quantum calculation, molecular docking, molecular dynamic, ADMET, QSAR, Heliyon, 9 (6) (2023) e16222.

[18] A. Singh, K.R. Ansari, M.A. Quraishi, S. Kaya, Theoretically and experimentally exploring the corrosion inhibition of N80 steel by pyrazol derivatives in simulated acidizing environment, Journal of Molecular Structure 1206 (127685) (2020) 1-12.

[19] J. Zhao, Z. Wang, P. Guo, Q. Luo, Molecular level investigation of methane and carbon dioxide adsorption on SiO_2 surface, Computational Materials Science 168 (2019) 213–220.

[20] H. Farrokhpour, H. Hadadzadeh, K. Eskandari, M. Movahedi, H. Jouypazadeh, van der Waals DFT ONIOM study of the adsorption of DNA bases on the Cu(111) nanosurface, Applied Surface Science, 422 (2017) 372-387.

[21] M. Esmaeilzadeh Khabazi, A. Najafi Chermahini, DFT Study on Corrosion Inhibition by Tetrazole Derivatives: Investigation of the Substitution Effect, ACS omega, 8 (11) (2023) 9978-9994.

[22] A.M. Ayuba, A. Uzairu, H. Abba, G.A. Shallangwa, Hydroxycarboxylic acids as corrosion inhibitors on aluminium metal: a computational study, Journal of Materials and Environmental Sciences, 9 (11) (2018) 3026-3034.

[23] M. Frisch, G. Trucks, H. Schlegel, G. Scuceria, M. Robb, J. Cheeseman, J. Pople, Gaussian 03, revision A.1; Gaussian, Inc.: Pittsburg, PA, Gaussian, Wallingford, CT, 2003.

[24] R.D. Dennington, T.A. Keith, J.M. Millam, Gauss View 5.0, Gaussian, 8 (2008).

[25] G. Gece, S. Bilgiç, A computational study of two hexitol borates as corrosion inhibitors for steel, International Journal of Corrosion and Scale Inhibition, 6 (4) (2017) 476–484.

[26] G. Gece, S. Bilgiç, Molecular-Level Understanding of the Inhibition Efficiency of Some Inhibitors of Zinc Corrosion by Quantum Chemical Approach, Industrial & Engineering Chemistry Research, 51 (43) (2012) 14115-14120.

[27] R. Hsissou, S. Abbout, R. Seghiri, M. Rehioui, A. Berisha, H. Erramli, M. Assouag, A. Elharfi, Evaluation of corrosion inhibition performance of phosphorus polymer for carbon steel in [1 M] HCl: Computational studies (DFT, MC and MD simulations), Journal of Materials Research and Technology, 9 (3) (2020) 2691-2703.

[28] V.T. Koopmans, Ordering of wave functions and e energies to the individual electrons of an atom Physica, 1 (1933).

[29] L. Pauling, The nature of the chemical bond Cornell University Press, London, 1960.

[30] R.G. Pearson, Absolute electronegativity and hardness: application to inorganic chemistry, Inorganic Chemistry, 27 (4) (1988) 734–740.

[31] S. Hadisaputra, A.D. Irham, A.A. Purwoko, E. Junaidi, A. Hakim, Development of QSPR models for furan derivatives as corrosion inhibitors for mild steel, International Journal of Electrochemical Science, 18 (8) (2023) 100207.

[32] H.R. Obayes, G.H. Alwan, A.H.M. Alobaidy, A.A. Al-Amiery, A.A. HKadhum, a.A.B. Mohamad, Quantum chemical assessment of benzimidazole derivatives as corrosion inhibitors, Chemistry Central Journal, 8 (21) (2014) 1-8.

[33] O.E. Oyeneyin, N.D. Ojo, N. Ipinloju, E.B. Agbaffa, A.V. Emmanuel, Investigation of the corrosion inhibition potentials of some 2-(4-(substituted) arylidene)-1H-indene-1,3-dione derivatives: density functional theory and molecular dynamics simulation, Beni-Suef University Journal of Basic and Applied Sciences, 11 (32) (2022).

[34] S. Hadisaputra, A.A. Purwoko, Y. Wirayani, M. Ulfa, S. Hamdiani, Density functional and perturbation calculation on the corrosion inhibition performance of benzylnicotine and its derivatives, 2243 (2020) 020006.

[35] D. Kumar, V. Jain, B. Rai, Imidazole derivatives as corrosion inhibitors for copper:

A DFT and reactive force field study, Corrosion Science 171 (108724) (2020) 1-9.

[36] E.E. Oguzie, C.B. Adindu, C.K. Enenebeaku, C.E. Ogukwe, M.A. Chidiebere, Kanayo, Natural Products for Materials Protection: Mechanism of Corrosion Inhibition of Mild Steel by Acid Extracts of Piper guineense, J. Phys. Chem. C 116 (2012) 13603−13615.

[37] M. Rajendran, K. Keerthika, M. Kowsalya, D. Devapiriam, Theoretical studies on corrosion inhibition efficiency of pyridine carbonyl derivatives using DFT method, Der Pharma Chemica, 8 (3) (2016) 71-79.

[38] F. Ramadhani, Emriadi, Syukri, Theoretical Study of Xanthone Derivative Corrosion Inhibitors Using Density Functional Theory (DFT), Jurnal Kimia Valensi, 6 (1) (2020) 95-103.

[39] D.R. Gusti, Emriadi, A. Alif, M. Efdi, Surface Characteristics on Mild Steel Using Aqueous Extract of Cassava (*Manihot esculenta*) Leaves as a Corrosion Inhibitor, Der Pharma Chemica, 8 (17) (2016) 113-118.

[40] H. Bourzi, R. Oukhrib, B. El Ibrahimi, H. Abou Oualid, Y. Abdellaoui, B. Balkard, S. El Issami, M. Hilali, L. Bazzi, C. Len, Furfural Analogs as Sustainable Corrosion Inhibitors—Predictive Efficiency Using DFT and Monte Carlo Simulations on the Cu(111), Fe(110), Al(111) and Sn(111) Surfaces in Acid Media, Sustainability, 12 (8) (2020) 3304.

[41] A. Khadiri, A. Ousslim, K. Bekkouche, A. Aouniti, I. Warad, A. Elidrissi, B. Hammouti, F.B. ·, M. Bouachrine, A. Zarrouk, 4-(2-(2-(2-(2-(Pyridine-4-yl)ethylthio)ethoxy)ethylthio)ethyl)pyridine as New Corrosion Inhibitor for Mild Steel in 1.0 M HCl Solution: Experimental and Theoretical Studies, Journal of Bio- and Tribo-Corrosion, 4 (64) (2018).

[42] M. Barbouchi, B. Benzidia, A. Ghaleb, A. Aouidate, M.E. Idrissi, M.b. Choukrad, Theoretical and Experimental Studies of Lentisk Leaf Extract as Green Corrosion Inhibitor for Iron in Chloride Media, Biointerface Research in Applied Chemistry, 13 (6) (2023).